126423-07-2; $[NCr(T\text{-}4\text{-}F\text{-}PP)]^{2-}$, 126423-17-4; $[NCr(T\text{-}4\text{-}Cl\text{-}PP)]^{+}$, 126422-90-0; $[NCr(T\text{-}4\text{-}Cl\text{-}PP)]$, 126422-97-7; $[NCr(T\text{-}4\text{-}Cl\text{-}PP)]^{-}$, 126423-08-3; $[NCr(T\text{-}4\text{-}Cl\text{-}PP)]^{2-}$, 126423-18-5; $[NCr(T\text{-}4\text{-}CF_3\text{-}PP)]^{+}$, 126422-91-1; $[NCr(T\text{-}4\text{-}CF_3\text{-}PP)]$, 126422-98-8; $[NCr(T\text{-}4\text{-}CF_3\text{-}PP)]^{-}$, 126423-09-4; $[NCr(T\text{-}4\text{-}CF_3\text{-}PP)]^{2-}$, 126423-19-6; $[NCr(T\text{-}4\text{-}CN\text{-}PP)]^{+}$, 126422-92-2; $[NCr(T\text{-}4\text{-}CN\text{-}PP)]$, 126422-99-9; $[NCr(T\text{-}4\text{-}CN\text{-}PP)]^{-}$, 126423-10-7; $[NCr(T\text{-}4\text{-}CN\text{-}PP)]^{2-}$, 126423-20-9; $[NCr(OEP)]^{+}$, 126423-22-1; $[NCr(OEP)]$, 84174-29-8; $[NCr(OEP)]^{-}$, 126423-23-2; $[NCr(OEP)]^{2-}$, 126541-09-1; $(CF_3CC(O)N)Mn(TPP)$, 126423-21-0; NMn(OEP), 84206-82-6; AA, 108-24-7; MCAA, 541-88-8; DCAA, 4124-30-5; TCAA, 4124-31-6; TFAA, 407-25-0; $(T\text{-}4\text{-}OCH_2Ph\text{-}PP)$, 17260-17-2; $(T\text{-}F\text{-}OCH_3\text{-}PP)$, 22112-78-3; $(T\text{-}4\text{-}CH_3\text{-}PP)$, 14527-51-6; (TPP), 917-23-7; (T-4-F-PP), 37095-43-5; (T-4-Cl-PP), 22112-77-2; nitride, 18851-77-9.

Contribution from the Department of Chemistry, Southwest Texas State University, San Marcos, Texas 78666, and Department of Chemical and Biological Sciences, Oregon Graduate Institute of Science and Technology, Beaverton, Oregon 97006-1999

# Resonance Raman Spectra of High- and Low-Spin Ferric Phenolates. Models for Dioxygenases and Nitrile Hydratase

Carl J. Carrano,*[1a] Mary W. Carrano,[1a] Kamala Sharma,[1b] Gabriele Backes,[1b] and Joann Sanders-Loehr*[1b]

*Received August 30, 1989*

A series of ferric phenolate complexes with Schiff base or methylamine substitutents ortho to the phenolic oxygen have been investigated. These include complexes with *N,N'*-ethylenebis((*o*-hydroxyphenyl)glycine), e.g., Na[Fe(EHPG)]; *N*-[2-(*o*-salicylideneamino)ethyl](*o*-hydroxyphenyl)glycine, e.g., $[Fe(EHGS)(X)_n]$, where $(X)_n = OH^-$, $H_2O$, or $(CN^-)_3$; and $N^1,N^4$-disalicylidenetriethylenetetramine, e.g., $[Fe((sal)_2trien)](PF_6)$. Although the majority of the complexes contained high-spin Fe(III), two low-spin species were generated: $[Fe((sal)_2trien)](PF_6)$ at 90 K and $[Fe(EHGS)(CN)_3]^{3-}$. Upon excitation within the phenolate → Fe(III) CT band, the resonance Raman spectra of both the high- and low-spin complexes are dominated by a set of phenolate vibrational modes at approximately 615, 630, 895, 1120, 1280, 1330, 1450, 1475, 1560, and 1600 $cm^{-1}$. The Schiff base containing ligands exhibit an additional resonance-enhanced vibration due to $\nu(C{=}N)$ at ~1640 $cm^{-1}$. The approximate doubling in the number of resonance-enhanced modes compared to the number in the Raman spectra of iron tyrosinate proteins is a consequence of the lower symmetry of ortho- relative to para-substituted phenolates. A correlation between Fe–O(phenolate) bond length with the intensity and/or frequency of the ~600-$cm^{-1}$ Fe–O stretching mode is proposed to explain the variability in the energy and intensity of the $\nu$(Fe–O) mode in iron tyrosinate proteins. The primary consequence of the formation of a low-spin state is to shift the phenolate → Fe(III) CT band from ~480 to ~650 nm, on the basis of the corresponding shift in the enhancement maximum of the ferric phenolate vibrational modes.

## Introduction

Iron tyrosinate proteins are now recognized as a distinct class of nonheme proteins, which includes the transferrins, the purple acid phosphatases, and a number of aromatic ring cleaving dioxygenases.[2,3] These proteins all contain high-spin Fe(III) characterized by a $g = 4.3$ EPR signal and a strong absorption band in the 400–600-nm range ($\epsilon_M$ = 2000–4000 $M^{-1}$ $cm^{-1}$) due to a phenolate oxygen to iron charge-transfer (CT) transition. In addition, these proteins show characteristic resonance-enhanced phenolate vibrations which have proven to be a useful resonance Raman (RR) signature. More recently a subclass of these iron–tyrosinate proteins has been discovered that have low-spin Fe(III) in their active sites. This group includes the tricyano adduct of transferrin[4] and the dicyano adduct of protocatechuate 3,4-dioxygenase.[5] Comparison with several low-spin iron(III) phenolate model complexes, $[Fe(EHGS)(CN)_3]^{3-}$ and the low-temperature form of $[Fe((sal)_2trien)]^{+}$ (Figure 1), shows that the low-spin species are characterized by small magnetic moments ($\mu_{eff} \simeq 2.0\ \mu_B$), anisotropic $g \simeq 2$ EPR spectra, and absorption bands in the 600–750-nm range ($\epsilon_M \simeq 1000$).[6-8a] The enzyme nitrile hydratase has similar EPR ($g$ values of 2.28, 2.14, and 1.97) and electronic absorption ($\lambda_{max}$ at 712 nm, $\epsilon_M$ = 1400 per Fe) properties,[8b] indicating that this protein may also belong to the low-spin iron(III) tyrosinate category.[6]

The 600–750-nm absorption band that is associated with low-spin complexes has been assigned as phenolate → Fe(III) CT on the basis of optical electronegativity arguments.[6] However, direct evidence for this assignment has been lacking. For this reason, a number of high- and low-spin ferric phenolate complexes have been examined by resonance Raman spectroscopy. We have found a similar set of iron phenolate modes in both cases, but with some shift in frequencies and intensities for the low-spin complexes. The enhancement of intensities with red excitation shows that the visible absorption bands in low-spin iron phenolates are indeed phenolate oxygen to iron CT transitions and that resonance Raman spectroscopy provides a unique spectral signature which may be useful in identifying low-spin Fe(III) sites in iron proteins.

## Experimental Procedures

The ligands for the Fe(III) complexes used in this study are depicted in Figure 1. The meso and rac isomers of Na[Fe(EHPG)] were prepared and purified as previously described.[9a] The isomeric purity was checked by thin-layer chromatography on silica gel using the upper layer of a butanol/$H_2O$/acetic acid (4:5:1) mixture. The aquo and hydroxo complexes of Fe(EHGS) were also prepared by published procedures.[9b,10]

(1) (a) Southwest Texas State University. (b) Oregon Graduate Institute of Science and Technology.
(2) Que, L., Jr. In *Biological Applications of Raman Spectroscopy*; Vol. 3, Spiro, T. G., Ed.; Wiley: New York, 1988; Vol. 3, pp 491–521.
(3) (a) Harris, D. C.; Aisen, P. In *Iron Carriers and Iron Proteins*; Loehr, T. M., Ed.; VCH: New York, 1989; pp 239–351. (b) Sanders-Loehr, J. *Ibid.*, pp 373–466. (c) Que, L., Jr. *Ibid.*, pp 467–524.
(4) Swope, S. K.; Chasteen, N. D.; Weber, K. E.; Harris, D. C. *J. Am. Chem. Soc.* **1988**, *110*, 3835.
(5) Whittaker, J. W., Lipscomb, J. D. *J. Biol. Chem.* **1984**, *259*, 4487.
(6) Spartalian, K.; Carrano, C. J. *Inorg. Chem.* **1989**, *28*, 19.
(7) Tweedle, M. F.; Wilson, L. J. *J. Am. Chem. Soc.* **1976**, *98*, 4824.
(8) (a) Sakurai, H.; Tsuchiya, K.; Migita, K. *Inorg. Chem.* **1988**, *27*, 3877. (b) Sugiura, Y.; Kuwahara, J.; Nagasawa, T.; Yamada, H. *J. Am. Chem. Soc.* **1987**, *109*, 5848.
(9) (a) Patch, M. G.; Simolo, K. P.; Carrano, C. J. *Inorg. Chem.* **1983**, *22*, 2630. (b) Carrano, C. J.; Spartalian, K.; Appa Rao, G. V. N.; Pecoraro, V. L.; Sundaralingam, M. J. *J. Am. Chem. Soc.* **1985**, *107*, 1651.

0020-1669/90/1329-1865$02.50/0 

**Table I.** Raman Vibrational Modes in High- and Low-Spin Ferric Phenolate Complexes[a]

| high-spin (solid)[b] | | | | | high-spin (soln)[c] | | low-spin (soln)[d] | |
|---|---|---|---|---|---|---|---|---|
| *meso*-Fe(EHPG) | *rac*-Fe(EHPG) | Fe(HDP)$(Cl)_2$ | Fe(Pr-sal)$_2$(Cl) | Fe(EHGS)$(H_2O)$ | Fe(EHGS)(OH) | Fe((sal)$_2$trien) | Fe(EHGS)$(CN)_3$ | Fe((sal)$_2$trien) |
| 614 s | 602 s | 602 s | 619 vs | 606 s | 610 s | 612 vs | 628 vs | 622 vs |
| 633 | 632 s | 628 | | 633 | 630 | | | 635 |
| 827 | 826 | 789 | 815 | 825 | 825 | | | |
| 893 | 895 | 888 | 883 | 896 | 893 | 900 | 911 | 900 |
| 1050 | 1028 | | 917 | | | | | 1005 |
| 1112 | 1110 | 1112 | 1125 | 1122 | 1125 | 1127 | 1014 | 1134 |
| 1154 | 1155 | 1153 | 1160 | 1153 | 1197 | 1150 | 1214 | 1257 |
| 1270 s | 1283 s | 1284 s | 1313 s | 1286 s | 1302 s | 1311 s | 1301 s | 1305 s |
| | 1330 | | 1336 | 1326 | 1331 | 1337 s | 1336 | 1344 s |
| 1366 | 1355 | | | 1351 | 1364 | | | |
| 1454 | 1456 | 1454 | 1441 | 1454 | 1454 | 1449 s | 1445 s | 1444 s |
| 1478 s | 1479 s | 1475 s | 1474 | 1478 s | 1479 s | 1472 | | |
| 1565 | 1564 | 1565 | | 1561 | 1567 | | 1551 | |
| 1596 s | 1595 s | 1593 s | 1599 s | 1600 s | 1600 s | 1602 s | 1600 s | 1603 s |
| | | | 1624 s | 1649 s | 1641 | 1630 s | | |

[a] Frequencies in $cm^{-1}$; s = strong, vs = very strong. [b] Solid samples were at 298 K in a spinning sample holder. Na[Fe(EHPG)], Fe(EHGS)$(H_2O)$, and Fe(Pr-sal)$_2$Cl were mixed with a 4–10-fold excess of KBr and analyzed with 488.0-nm excitation. Fe(HDP)$Cl_2$ was mixed with a 3-fold excess of $Na_2SO_4$ and analyzed with 514.5-nm excitation. [c] Solution samples in capillaries analyzed with 488.0-nm excitation. $[Fe(EHGS)(OH)]^-$ was in 20% DMSO in water (pH reading 9.1) at 90 K. [Fe((sal)$_2$trien)]$(PF_6)$ was in acetonitrile at 298 K. [d] Solution samples in capillaries analyzed with 647.1-nm excitation. $[Fe(EHGS)(CN)_3]^{3-}$ was in 10% DMSO in water, 1 M NaCN (pH 8.0), at 90 K. [Fe((sal)$_2$trien)]$(PF_6)$ was in acetonitrile at 90 K.

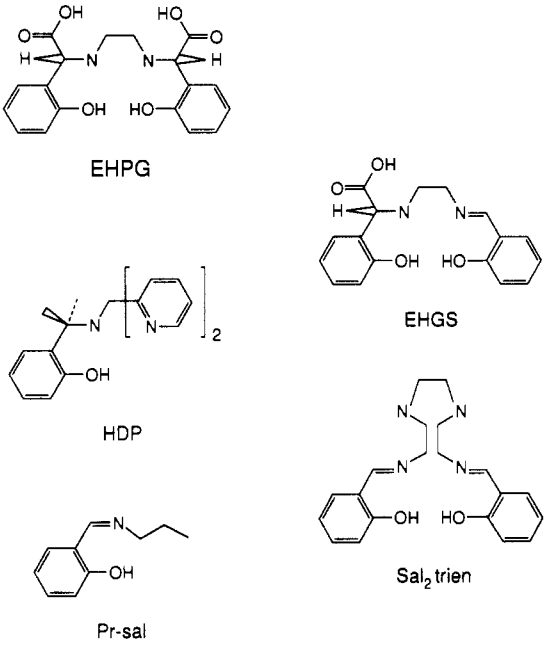


**Figure 1.** Principal coordinating ligands for ferric complexes used in this study. EHPG = tetraanion of *N*,*N*′-ethylenebis((*o*-hydroxyphenyl)-glycine), EHGS = trianion of *N*-[2-(*o*-salicylideneamino)ethyl](*o*-hydroxyphenyl)glycine, (sal)$_2$trien = dianion of $N^1$,$N^4$-disalicylidenetriethylenetetramine, HDP = anion of *N*-(*o*-hydroxybenzyl)-*N*,*N*-bis(2-pyridylmethyl)amine, and Pr-sal = anion of *N*-propylsalicylideneamine.

The Fe(III) complex derived from triethylenetetramine and salicylaldehyde, [Fe(sal)$_2$trien]$(PF_6)$, was synthesized by the method of Tweedle and Wilson[7] and purified by crystallization from methylene chloride/hexane. The low-spin tricyano complex[6] of Fe(EHGS) was prepared by the addition of an equimolar volume of 2 M NaCN (pH 8.0) to $[Fe(EHGS)(OH)]^-$ in 20% DMSO (pH reading 9.1) to give a final concentration of $4.8 \times 10^{-3}$ M at pH 8.0. The mixture was aged for 80 min and the resulting deep green solution had the expected absorbance at 690 nm for $\epsilon_M = 1200$. The following compounds were generously provided: Fe(Pr-sal)$_2$Cl,[11a] Bruce A. Averill; Fe(HDP)$Cl_2$ and $[Fe_2O(HDP)_2(OBz)](BPh_4)$,[11b] Lawrence Que, Jr.

Raman spectra were recorded on a computerized Jarrell-Ash spectrophotometer using Spectra-Physics 164-05 (Ar) and 2025-11 (Kr) lasers. Solid samples were examined with an ~150° backscattering geometry in a rotating sample holder at room temperature or, for frozen samples, in a capillary cooled to 90 K inside a copper cold finger in a Dewar flask. Solution samples at room temperature were studied in capillaries with a 90° scattering geometry. All spectra were obtained with a resolution of 6 $cm^{-1}$ and a scan rate of 1 $cm^{-1}/s$. Raman frequencies have been corrected by using an indene standard[12] and are accurate to ±1 $cm^{-1}$.

## Results

**High-Spin Complexes.** Normal high-spin iron tyrosinate proteins show four characteristic resonance Raman (RR) peaks at approximately 1170, 1280, 1500, and 1600 $cm^{-1}$ upon excitation into the ~490-nm Tyr → Fe CT band.[2] The features at 1170 and 1280 $cm^{-1}$ are assigned to C–H bending and C–O stretching modes, respectively, whereas the features at 1500 and 1600 $cm^{-1}$ are assigned to ring C=C stretching modes.[2] A peak at ~600 $cm^{-1}$ is also frequently observed and is thought to be the Fe–O-(phenolate) stretch although containing considerable ring vibrational character as well.[13] A similar set of five peaks has been observed at 568, 1168, 1272, 1501, and 1603 $cm^{-1}$ for the *p*-cresol moiety in the Fe(salen)$(OC_6H_4$-4-$CH_3)$ complex.[13] However, the RR spectrum of Na[Fe(EHPG)] with its ortho-substituted phenolate moiety was found to be considerably more complex.[14] The spectrum is still dominated by four of the five phenolate modes at ~600, 1280, 1480, and 1600 $cm^{-1}$. However, most of these peaks show evidence of splitting into additional spectral components.

The previously reported[14] RR spectrum of Na[Fe(EHPG)] was obtained on an unresolved mixture of isomers. Since that time, X-ray crystallography has demonstrated that crystals of Na-[Fe(EHPG)] contain two isomers.[15] In both cases, the phenolates are cis to one another, but the meso isomer has cis carboxylates and inequivalent phenolates, whereas the racemic isomer has trans carboxylates and $C_2$ symmetry. The resolved meso and racemic isomers of Na[Fe(EHPG)] show quite similar RR spectra (Figure 2). For example, both have intense $\nu$(C=C) modes near 1478 and 1595 $cm^{-1}$ with smaller features at ~1455 and ~1565 $cm^{-1}$. Thus, the appearance of multiple peaks cannot be ascribed to contributions from different isomers but must rather be due to a constant structural feature of these molecules. Furthermore, the spectral splitting of phenolate modes is no greater for the meso isomer, despite the fact that the molecule has inequivalent phenolates with Fe–O distances of 1.893 and 1.922 Å compared to

(10) Spartalian, K.; Carrano, C. J. *Inorg. Chem.* **1984**, *23*, 1993.
(11) (a) Davies, J. E.; Gatehouse, B. M. *Acta Crystallogr., Sect. B* **1972**, *B28*, 3541. (b) Yan, S.; Que, L., Jr.; Taylor, L. F.; Anderson, O. P. *J. Am. Chem. Soc.* **1988**, *110*, 5222.
(12) Hendra, P. J.; Loader, E. J. *Chem. Ind.* **1968**, 718.
(13) Pyrz, J. W.; Roe, A. L.; Stern, L. J.; Que, L., Jr. *J. Am. Chem. Soc.* **1985**, *107*, 614.
(14) Gaber, B. P.; Miskowski, V.; Spiro, T. G. *J. Am. Chem. Soc.* **1974**, *96*, 6868.
(15) Bailey, N. A.; Cummins, D.; McKenzie, E. D.; Worthington, J. M. *Inorg. Chim. Acta* **1981**, *50*, 111.

**Table II.** Spectroscopic and Metric Properties of the Ferric Phenolate Complexes

| no. | complex[a] | $\lambda_{max}$ ($\epsilon_M$)[b] | bond length, Å[c] Fe—O | bond length, Å[c] C—O | Fe–O–C angle, deg[c] | frequency, $cm^{-1}$[a] $\nu$(Fe—O) | frequency, $cm^{-1}$[a] $\nu$(C—O) | intensity ratio[d] $\nu$(Fe–O)/$\nu$(C=C) | $I_{647}/I_{488}$[e] $\nu$(Fe—O) | $I_{647}/I_{488}$[e] $\nu$(C=C) |
|---|---|---|---|---|---|---|---|---|---|---|
| | | | | | High-Spin State | | | | | |
| 1 | $Fe_2O(HDP)_2(OBz)^+$ | 522 (6600) | 1.928 | 1.310 | 130.1 | 598 | 1299 | 1.3 | | |
| 2 | $Fe(HDP)Cl_2$ | 590 (2100) | | | | 602 | 1284 | 2.6 | | |
| 3 | *rac*-Fe(EHPG) | 475 (4500) | 1.904 | 1.36 | 129.5 | 602 | 1283 | 0.8 | | |
| 4 | *meso*-Fe(EHPG) | 486 (4100) | 1.908 | 1.355 | 130.1 | 614 | 1270 | 1.2 | | |
| 5 | $Fe(EHGS)(OH^-)$ | 440 (2900) | | | | 610 | 1302 | 1.3 | 0.2 | 0.2 |
| 6 | $Fe(EHGS)(H_2O)$ | 497 (4000) | 1.899 | | | 606 | 1286 | 1.1 | | |
| 7 | $Fe((sal)_2trien)^+$ | 490 (3600) | | | | 612 | 1311 | 2.5 | 0.2 | 0.4 |
| 8 | $Fe(Pr\text{-}sal)_2Cl$ | 460 (3100) | 1.89 | 1.31 | | 619 | 1313 | 3.8 | | |
| | | | | | Low-Spin State | | | | | |
| 9 | $Fe(EHGS)(CN^-)_3$ | 690 (1200) | | | | 628 | 1301 | 3.4 | 5 | |
| 10 | $Fe((sal)_2trien)^+$ | 620 (1900) | 1.883 | 1.322 | | 622 | 1305 | 4.5 | 24 | 13 |

[a] Sample and Raman spectral conditions as described in Table I. [b] $\lambda_{max}$ in nm, $\epsilon$ in $M^{-1}$ $cm^{-1}$ from following sources: sample **1** from ref 11c, samples **5**, **6**, and 9 from ref 6, sample **7** from ref 7, samples **3** and **4** in $H_2O$ and samples **2** and **8** in acetonitrile from this work. [c] Average bond lengths and bond angles from the following sources: $[Fe_2O(HDP)_2(OBz)](ClO_4)$ from ref 11b, Na[Fe(EHPG)] isomers from ref 15, $Fe(EHGS)(CH_3OH)$ from ref 9b assumed to be equivalent to $Fe(EHGS)(H_2O)$, low-spin $Cl^-$ and $NO_3^-$ salts of $[Fe((sal)_2trien)]^+$ from ref 20 assumed to be equivalent to low-spin $[Fe((sal)_2trien)](PF_6)$. [d] Intensity of $\nu$(Fe–O) relative to $\nu$(C=C) at 1594–1603 $cm^{-1}$ measured with 488.0-nm excitation for high-spin complexes (514.5 nm for $Fe(HDP)Cl_2$) and with 647.1-nm excitation for low-spin complexes. Intensities are based on peak heights, owing to the sharpness and high resolution of the phenolate modes. [e] Intensity ratio for excitation at 647.1 vs 488.0 nm was obtained on a single sample in a sealed capillary. Sample peak heights for $\nu$(Fe–O) and the ~1600-$cm^{-1}$ $\nu$(C=C) were quantitated relative to solvent internal standards ($CH_3CN$ peak at 932 $cm^{-1}$ for samples **7** and **10** and DMSO peak at 678 $cm^{-1}$ for samples **6** and **9**).

a single Fe–O distance of 1.904 Å in the racemic isomer.

The major structural features that differentiate the Na[Fe(EHPG)] complexes from the iron tyrosinate complexes are that they are ortho- rather than para-substituted phenolates. A number of other phenolate ligands containing either –C=N or –C—NH in the ortho position and with either one or two phenolates per Fe give surprisingly RR spectra similar to those of the Na[Fe(EHPG)] complexes (Table I). These include the imino derivatives, $[Fe((sal)_2trien)](PF_6)$[7] and $Fe(Pr\text{-}sal_2)Cl$;[11a] the –C—NH derivative, Fe(HDP)Cl;[11b] and a derivative containing both –C=N and –C—NH functionalities, Fe(EHGS).[9b] Typical spectra are shown for $Fe(EHGS)(H_2O)$ in Figure 2C and for $[Fe((sal)_2trien)](PF_6)$ in Figure 3A. Common features are the presence of four intense modes at 602–619, 1270–1313, 1472–1479, and 1594–1602 $cm^{-1}$. There is also another set of six somewhat weaker features at 626–633, 883–900, 1110–1127, 1326–1337, 1441–1456, and 1561–1567 $cm^{-1}$. As in the metal tyrosinate proteins and model compounds,[2,16] the $\nu$(C–O) mode at 1270–1313 $cm^{-1}$ is the most variable and the most sensitive to the environment of the complex.

The spectra of the $H_2O$ and $OH^-$ complexes of Fe(EHGS) were also obtained in aqueous solutions at pH readings of 5.7 and 9.1, respectively, with 20% DMSO added to increase the solubility of the samples. Data for the $[Fe(EHGS)(OH)]^-$ complex are given in Table I and Figure 4A. The solution spectrum for $Fe(EHGS)(H_2O)$ is essentially indistinguishable from that of the hydroxide complex (data not shown). The major difference between the solid and solution states is the shift of the $\nu$(C–O) mode from 1287 to 1302 $cm^{-1}$. The similarity in the phenolate vibrational modes for the aquo and hydroxo forms in aqueous solution is surprising in view of the substantial blue shift in the Tyr → Fe CT transition (Table II) upon hydrolysis of the coordinated water molecule. This behavior is reminiscent of the diiron-containing acid phosphatases where the color of the chromophoric Fe(III) changes from purple to pink in response to changes in iron ligands such as phosphate with very little effect on the RR spectrum of the iron tyrosinate chromophore.[17]

The fact that the same RR features are observed for a number of different complexes indicates that these are all vibrations of the phenolate moiety. The only other structural component that can be detected in the RR spectrum is the –C=N substituent.

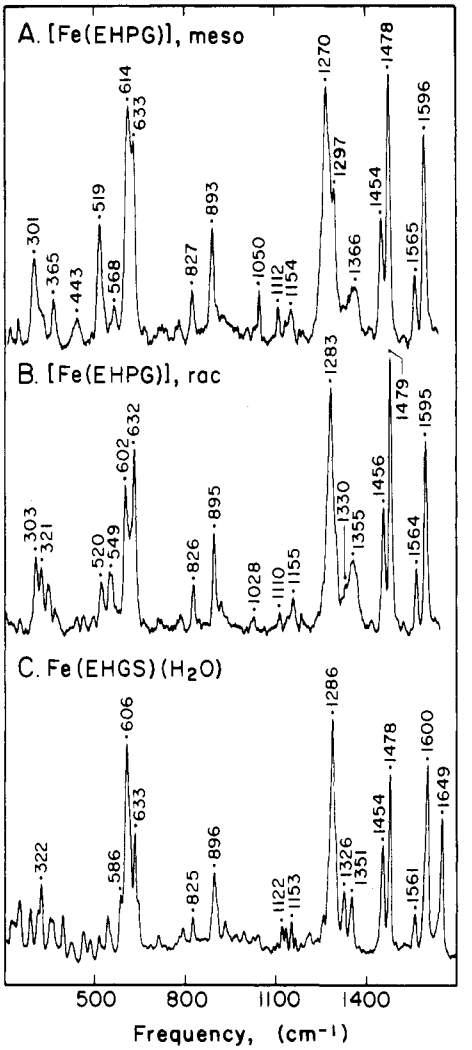


**Figure 2.** Resonance Raman spectra of high-spin ferric phenolate complexes in the solid state: (A) *meso* isomer of Na[Fe(EHPG)]; (B) *rac* isomer of Na[Fe(EHPG)]; (C) $Fe(EHGS)(H_2O)$. Samples were mixed with a 10-fold excess of KBr and analyzed in a spinning sample holder at room temperature. Spectra were obtained with 488.0-nm excitation, 75 mW, and an average of 9–12 scans.

The C=N stretch characteristic of this group[18] appears between 1624 and 1649 $cm^{-1}$ in all of the high-spin complexes containing

(16) Sharma, K. D.; Andersson, L. A.; Loehr, T. M.; Terner, J.; Goff, H. M. *J. Biol. Chem.* **1989**, *264*, 12772.

(17) (a) Averill, B. A.; Davis, J. C.; Burman, S.; Zirino, T.; Sanders-Loehr, J.; Loehr, T. M.; Sage, J. T.; Debrunner, P. G. *J. Am. Chem. Soc.* **1987**, *109*, 3760. (b) Backes, G.; Sanders-Loehr, J.; Loehr, T. M.; David, S.; Que, L., Jr. Unpublished results.

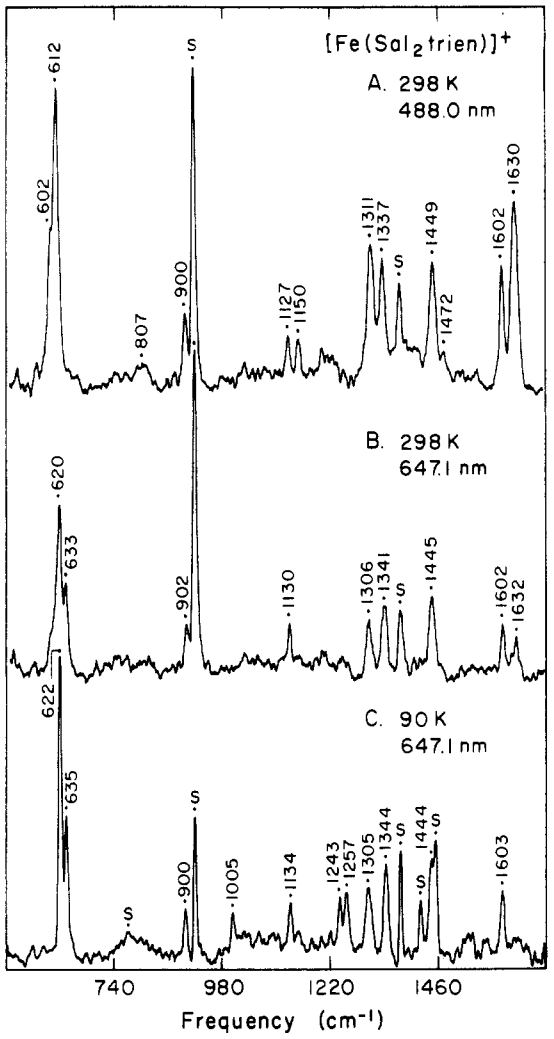


**Figure 3.** Resonance Raman spectra of $[Fe((sal)_2trien)](PF_6)$ dissolved in acetonitrile (solvent peaks denoted by S): (A) sample at 298 K in capillary (spectrum obtained via 90° scattering with 50 mW of 488.0-nm excitation (4 scans)); (B) conditions as in (A) but with 35 mW of 647.1-nm excitation (9 scans); (C) conditions as in (B) but with sample in capillary at 90 K and data collection via 150° backscattering.

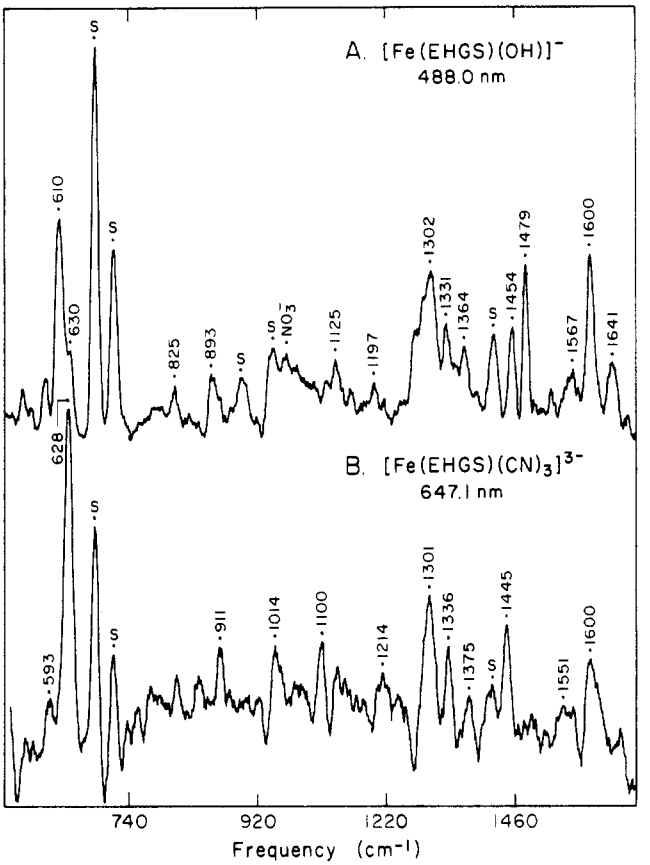


**Figure 4.** Resonance Raman spectra of Fe(EHGS) complexes in aqueous solution: (A) $[Fe(EHGS)(OH)]^-$, $10^{-2}$ M, in 20% DMSO and 0.2 M $KNO_3$ at a pH reading of 9.1 (spectrum obtained on sample at 90 K by using 488.0-nm excitation, 75 mW (4 scans)); (B) $[Fe(EHGS)(CN)_3]^{3-}$, $0.5 \times 10^{-2}$ M, in 1 M NaCN, 10% DMSO, and 0.1 M $KNO_3$ at a pH reading of 8.0 (spectrum obtained on sample at 90 K by using 647.1-nm excitation, 45 mW (16 scans)).

this functionality (Table I) and is quite strongly enhanced (Figures 2C and 3A). This suggests that the imino nitrogen coordinated to the iron contributes to the LMCT transition being probed.

The phenolate vibrational intensities in the high-spin Fe(III) complexes are resonance enhanced by excitation within the phenolate → Fe(III) CT band at ~500 nm (Table II). When the excitation wavelength is changed to 647 nm, there is a marked drop in ferric phenolate peaks relative to the solvent peaks. Quantitation based on peak heights shows an ~5-fold decrease in intensity on going from 488- to 647-nm excitation (Table II). This is the expected behavior since these complexes have much weaker absorbance in the 650-nm region.

**Low-Spin Complexes.** Addition of excess cyanide to Fe(EHGS) at pH 8.0 results in the formation of the low-spin species, $[Fe(EHGS)(CN)_3]^{3-}$.[6] Excitation within its 690-nm absorption band results in a RR spectrum typical of ferric phenolates, with intense features at 628, 1301, 1336, 1445, and 1600 $cm^{-1}$ (Figure 4B, Table I). The most prominent spectral difference between the high- and low-spin forms of Fe(EHPG) is the shift in $\nu$(Fe–O) from ~610 and 628 $cm^{-1}$ and the 2–3-fold increase in its intensity relative to the other phenolate modes (Figure 4). The increase in frequency is most likely the results of Fe–O bond shortening and suggests that the cyanide ligands (well-known for their trans-labilizing effects)[19] must be located cis to the phenolate oxygens. The 690-nm absorption band in $[Fe(EHGS)(CN)_3]^{3-}$ was previously assigned as phenolate → low-spin Fe(III) CT on the basis of Jorgenson's optical electronegativity theory.[6] This is now confirmed by the RR behavior of the 628-$cm^{-1}$ $\nu$(Fe–O) mode which is 5-fold more strongly enhanced with 647- than with 488-nm excitation (Table II).

The $[Fe((sal)_2trien)](PF_6)$ complex is known to undergo a change in spin state with temperature.[7] This behavior provides a unique opportunity to compare the RR spectra of a high- and low-spin ferric phenolate with *identical* iron ligands. In acetone or acetonitrile at ~310 K, $[Fe(sal_2trien)](PF_6)$ is predominantly high spin ($\mu_{eff}$ = 5.0 $\mu_B$), whereas at 200 K it is low spin ($\mu_{eff}$ = 1.8 $\mu_B$).[7] This high-spin to low-spin interconversion can be followed by optical spectroscopy in acetone.[7] At ~310 K, the complex has its major absorption at 490 nm ($\epsilon_M$ = 3600) with a small shoulder at 620 nm. At ~250 K, the major absorption is at 620 nm ($\epsilon_M$ = 1900) with a small shoulder at 490 nm. The resonance Raman behavior is entirely in accord with these observations.

For $[Fe((sal)_2trien)](PF_6)$ in acetonitrile at room temperature (298 K), excitation with 488 nm produces a Raman spectrum characteristic of high-spin iron(III) phenolates with intense peaks at 612, 1311, 1449, and 1602 $cm^{-1}$ (Figure 3A). After freezing of the sample to 90 K, the best RR spectrum is obtained with red excitation (Figure 3C). This spectrum shows a similarity to the $[Fe(EHGS)(CN)_3]^{3-}$ spectrum in that the $\nu$(Fe–O) mode has increased in intensity and shifted to 622 $cm^{-1}$, while the $\nu$(C=N) mode at 1630 $cm^{-1}$ has disappeared (Table I). The increase in energy for $\nu$(Fe–O) is consistent with the observed shortening of

(18) Dollish, F. R.; Fateley, W. G.; Bentley, F. F. *Characteristic Raman Frequencies of Organic Compounds*; John Wiley: New York, 1974.

(19) Cotton, F. A.; Wilkinson, G. *Advanced Inorganic Chemistry*; John Wiley: New York, 1980; p 1200.

Fe–L bond lengths in low-spin $[Fe((sal)_2trien)]^+$ complexes.[20] The other phenolate modes, particularly $\nu$(C–O) at ~1300 $cm^{-1}$, are at energies similar to those of the high-spin complexes in solution. The ferric phenolate modes in $[Fe((sal)_2trien)](PF_6)$ at 298 K are 2.5- to 5-fold more enhanced with 488- than 647-nm excitation, whereas, at 90 K, they are 13- to 24-fold more enhanced with 647- than 488-nm excitation (Table II). This provides conclusive evidence that the observed spectra represent high-spin and low-spin components, respectively.

The RR spectrum of the $[Fe((sal)_2trien)]^+$ complex in acetonitrile at 298 K obtained with 647-nm excitation is primarily that of the residual low-spin material in the sample (Figure 3B). The spectral peaks at 620, 633, and 1306 $cm^{-1}$, as well as the loss of intensity at 1632 $cm^{-1}$, are close to the properties of the low-spin complex (Figure 3C). Other observations that also indicate a substantial fraction of low-spin material for the dissolved complex at room temperature are the shoulder at 620 nm in the absorption spectrum and the low magnetic moment ($\mu_{eff}$ = 5.05 $\mu_B$) compared to that of the high-spin solid ($\mu_{eff}$ = 5.81 $\mu_B$).[7] Both the absorption and magnetic data suggest the presence of ~20% low-spin complex at room temperature. The fact that the phenolate modes in the Raman spectrum are 2.5 to 5 times more strongly enhanced with 488-nm excitation (selective for high-spin species) than with 647-nm excitation (selective for low-spin species) is in agreement with there being a relatively small amount of low-spin component. In contrast, the aqueous Fe(EHPG) complexes in the absence of cyanide show no indication of a low-spin component in either their room-temperature absorption spectra or their low-temperature EPR spectra (dominated by $g$ = 4.3 signal at 77 K).[9b]

## Discussion

The resonance Raman spectra of ferric phenolate complexes with amine (–C—NH) or imine (–C=N) substituents ortho to the phenolate oxygen are considerably more complex than those of para-substituted phenolates[2,13] such as tyrosine or *p*-cresol. The *o*-phenolate complexes show seven to eight prominent features in the 1100–1600-$cm^{-1}$ region compared to the set of four peaks in this region for the *p*-phenolate complexes. The *o*-phenolate vibrational pattern is unaffected by the amine or imine nature of the *o*-substituent or by the number or geometrical arrangement of phenolate moieties in the complex. *The increased spectral complexity is explained by the lower symmetry of the o-phenolates.* In a study of a series of monosubstituted phenols, Green et al.[21a] reported approximately twice as many Raman bands for the *o*-substituted than for the *p*-substituted phenols (which still have $C_2$ symmetry). Similarly, monodentate ferric catecholates were found to have twice as many phenolate modes as the more symmetrical bidentate complexes.[13] The increased number of vibrational modes in the lower symmetry compounds is most likely a consequence of the lifting of degeneracies.

Although the vibrational spectra of substituted phenols have been fully assigned by using isotopic and other regularly varied substituents,[21a,b] no such rigorous investigations have been undertaken to assign the RR spectra of metal phenolate complexes. The present comparison of *o*-phenolate complexes reveals that the 600–1600-$cm^{-1}$ region of the RR spectrum contains 12–14 peaks that are characteristic of the *o*-phenolate moiety by virtue of their being present in the 9 different compounds investigated and their being in resonance with the phenolate → Fe(III) charge-transfer band. The only peak that may be definitively assigned is the intense $\nu$(C–O) mode near 1300 $cm^{-1}$, which has been observed to shift to lower energy in the RR spectra of a copper(II) *o*-phenolate complex[22] and an iron(III) *p*-phenolate complex[13] upon substitution with $^{18}O$-enriched phenolate. In the latter complex, an additional $^{18}O$-sensitive mode has been identified at 568 $cm^{-1}$ and assigned as having strong $\nu$(Fe–O) character. Neither of these vibrational modes would be expected to undergo splitting as a consequence of the lowered symmetry of an *o*-phenolate moiety.

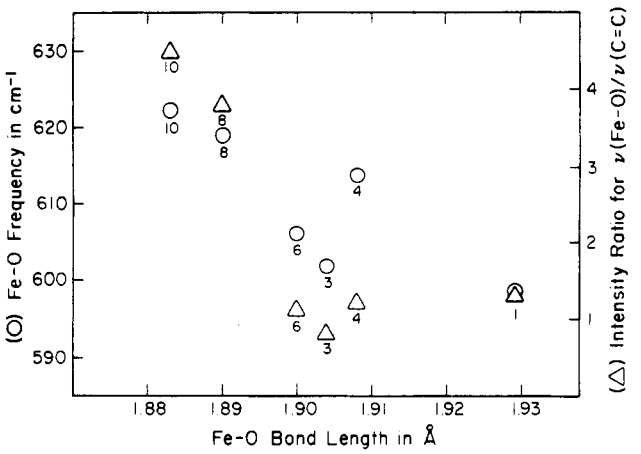


**Figure 5.** Correlation of Fe–O vibrational frequency and intensity with Fe–O bond length for ferric complexes with ortho-substituted phenolate ligands. Data are from Table II. The intensity of the Fe–O stretch is relative to the intensity of the C=C stretch at ~1600 $cm^{-1}$.

Additional evidence for the $\nu$(Fe–O) and $\nu$(C–O) assignments for the peaks near 600 and 1300 $cm^{-1}$, respectively, in the ferric *o*-phenolate complexes is that these two modes show the greatest variability in frequency. This phenomenon has been well documented for a number of metal phenolates, both in proteins and model systems with divalent or trivalent metal ions, where $\nu$(Fe–O) varies from 568 to 623 $cm^{-1}$ and $\nu$(C–O) varies from 1258 to 1316 $cm^{-1}$.[2,16] A further indication of $\nu$(Fe–O) character in the ~600-$cm^{-1}$ mode is that the vibrational frequency appears to increase with decreasing Fe–O bond length (Table II, Figure 5). Thus, the low-spin complexes with their shorter Fe–O distances have their $\nu$(Fe–O) modes at higher energy than the high-spin complexes. Similarly, a ferric porphyrin with with an axial phenolate, $[Fe(TTOP)]_2$, has a high 623-$cm^{-1}$ $\nu$(C–O), which corresponds to an unusually short 1.85-Å Fe–O bond length.[16] What is somewhat unexpected is that the *intensity* of the $\nu$(Fe–O) mode relative to the phenolate ring modes also seems to increase with decreasing Fe–O bond lengths (Figure 5). Thus, complexes with Fe–O bonds above 1.90 Å have $\nu$(Fe–O) to $\nu$(C=C) intensity ratios close to 1, whereas complexes with a shorter Fe–O bond of 1.88–1.89 Å have intensity ratios near 4.

The origin of the variability of the $\nu$(C–O) mode has been the subject of some speculation. As indicated in Table II, there is again a strong dependence on C–O bond strength such that larger vibrational frequencies are associated with shorter C–O bond distances. It had been suggested that this variability might be accounted for by the strength of the metal phenolate interaction, with weaker M–O bonds serving to increase the double-bond character of the C–O bond.[23] However, this is not observed for the *o*-phenolate complexes in Table II, where compounds **8** and **10**, for example, with shorter C–O distances also have shorter Fe–O distances. Instead there appears to be a correlation with the electron-withdrawing character of the ortho substituent. Complexes **7**–**10** with imino functionalities have shorter C–O bond lengths (1.31–1.32 Å) and larger $\nu$(C–O) values (1301–1313 $cm^{-1}$) than the amino complexes **2**–**4** with longer C–O bond lengths (1.35–1.36 Å) and smaller $\nu$(C–O) values (1270–1284 $cm^{-1}$). A similar observation has been made regarding the increase in $\nu$(C–O) to 1316 $cm^{-1}$ in a copper(II) trichlorophenolate complex due to the influence of the electron-withdrawing chloro groups.[22] Finally, it has been suggested that C–O vibrational frequencies above 1300 $cm^{-1}$ could be associated with an increase in the M–C–O(phenolate) angle from the expected ~120° to values of 130° or more.[22] This is not supported by the present in investigation where complexes **3** and **4** with Fe–C–O angles of 130° have $\nu$(C–O) vibrations at 1270–1283 $cm^{-1}$. A more likely ex-

(20) Sinn, E.; Sim, G.; Dose, E. V.; Tweedle, M. F.; Wilson, L. J. *J. Am. Chem. Soc.* **1978**, *100*, 3375.
(21) (a) Green, J. H. S.; Harrison, D. J.; Kynaston, W. *Spectrochim. Acta* **1971**, *27A*, 2199. (b) Jakobsen, R. J. *Spectrochim. Acta* **1965**, *21*, 433.
(22) Pyrz, J. W.; Karlin, K. D.; Sorrell, G. C.; Que, L., Jr. *Inorg. Chem.* **1984**, *23*, 4581.
(23) Tomimatsu, K.; Kint, S.; Scherer, J. R. *Biochemistry* **1976**, *15*, 4918.

planation for the variability, particularly in proteins which have the same tyrosinate ligands, is that the C-O bond strength is influenced by the environment of the metal phenolate moiety. An example of such behavior is observed for the Fe(EHGS)($H_2O$) complex, where $\nu$(C-O) occurs at 1286 $cm^{-1}$ in the solid material and at 1300 $cm^{-1}$ in aqueous solution with 20% DMSO.

Potential Fe-O stretching modes have been detected in the RR spectra of a number of iron tyrosinate proteins. These include the 575-$cm^{-1}$ vibration in purple acid phosphatase[17] as well as peaks at 578, 588, and 603 $cm^{-1}$ in three different mutant hemoglobins with axial tyrosinate ligands.[24] Nevertheless, in a number of other iron tyrosinate proteins such as transferrin,[25] protocatechuate 3,4-dioxygenase,[26] and catalase,[16,27] there is no peak in the 600-$cm^{-1}$ region of intensity comparable to that of the 1100-1600-$cm^{-1}$ phenolate modes. The inability to detect a $\nu$(Fe-O) mode in these proteins may be indicative of a fairly long Fe-O(tyrosinate) bond. This possibility is supported by the report of a 2.2-Å Fe-O bond length in *Penicillium vitale* catalase, based on the crystal structure at 2.0-Å resolution.[28]

Conversion of ferric phenolates from high-spin to low-spin states is generally accompanied by a decrease in Fe-O bond distance.[19] Thus, the low-spin complexes examined in this study had Fe-O frequencies of 622-628 $cm^{-1}$ (Table I), and their $\nu$(Fe-O) modes were 3.4-4.5-fold more intense than the ~1600-$cm^{-1}$ phenolate $\nu$(C=C) mode (Table II). A further distinguishing characteristic of the low-spin ferric phenolates is the marked red shift of the Tyr → Fe(III) CT band (Table II) and the selective enhancement of the phenolate vibrational modes upon excitation within the ~650-nm absorption band. Thus, RR spectroscopy could provide a useful method for identifying low-spin ferric phenolate sites in proteins.

The enzyme nitrile hydratase contains a low-spin Fe(III) site.[8b] Its EPR parameters are well matched by $Fe^{III}$ salen complexes with axial thiolate or imidazolate ligands.[8a] This finding, along with the 712-nm absorption maximum ($\epsilon_M$ = 1400 per Fe) in the enzyme, suggests the additional presence of phenolate ligands. Unfortunately, it has not yet been possible to obtain an RR spectrum of nitrile hydratase due to the large fluorescence of the protein.[29] We also observed markedly increased fluorescence for the low-spin $[Fe(EHGS)(CN)_3]^{3-}$ complex but not for the low-spin $[Fe((sal)_4trien)](PF_6)$ complex. In addition, the low-spin tricyano form of transferrin[4] has been found to be considerably more fluorescent than the native high-spin protein.[30] Thus, excessive fluorescence may interfere with the ability to detect phenolate vibrational modes in low-spin iron proteins by resonance Raman spectroscopy.

**Acknowledgment.** This work was supported by grants from the National Institutes of Health, GM 18865 (J.S.-L.), and the Research Corp. (C.J.C.).

(24) Nagai, M.; Yoneyama, Y.; Kitagawa, T. *Biochemistry* **1989**, *28*, 2418.
(25) Tomimatsu, Y.; Kint, S.; Scherer, J. R. *Biochem. Biophys. Res. Commun.* **1973**, *54*, 1067.
(26) Keyes, W. E.; Loehr, T. M.; Taylor, M. L. *Biochem. Biophys. Res. Commun.* **1978**, *83*, 941.
(27) Chuang, W.-J.; Johnson, S.; Van Wart, H. E. *J. Inorg. Biochem.* **1988**, *34*, 201.
(28) Melik-Adamyan, W. R.; Barynin, V. V.; Vagin, A. A.; Vainshtein, B. K.; Grebenko, A. I.; Borisov, V. V.; Bartels, K. S.; Fita, I.; Rossmann, M. G. *Sov. Phys.—Crystallogr. (Engl. Transl.)* **1987**, *32*, 372.
(29) Sugiura, Y.; Kitagawa, T. Personal communication.
(30) Han, Z.; Loehr, T. M.; Sanders-Loehr, J.; Grady, J.; Chasteen, N. D. Unpublished results.

Contribution from the School of Mathematical and Physical Sciences, Murdoch University, Perth, WA 6150, Australia, School of Chemistry, University of Bath, Bath BA2 7AY, U.K., and Department of Physics, University of Liverpool, Liverpool L69 3BX, U.K.

# Biomineralization of Iron: Mössbauer Spectroscopy and Electron Microscopy of Ferritin Cores from the Chiton *Acanthopleura hirtosa* and the Limpet *Patella laticostata*

T. G. St. Pierre,[†] K.-S. Kim,[1,†] J. Webb,*[,†] S. Mann,[‡] and D. P. E. Dickson[§]

*Received September 29, 1988*

Ferritins isolated from the hemolymph of the chiton *Acanthopleura hirtosa* and the limpet *Patella laticostata* have been studied by $^{57}Fe$ Mössbauer spectroscopy, electron diffraction, transmission electron microscopy (TEM), and inductively coupled plasma (ICP) spectrometry. Mössbauer spectra of the samples at 78 K were quadrupole-split doublets with similar quadrupole splittings and chemical isomer shifts, characteristic of octahedral high-spin iron(III), while at 4.2 K the spectra were magnetically split sextets. The spectra yield mean superparamagnetic blocking temperatures of about 32 and 30 K for the *A. hirtosa* and *P. laticostata* ferritins, respectively, and indicate magnetic ordering temperatures of about 37 and 34 K. Core size distributions were measured for both the *A. hirtosa* and *P. laticostata* ferritins by using TEM and gave mean core size ranges of 8.0-8.5 and 7.5-8.0 nm, respectively. Diffuse lines in the electron diffraction patterns of the ferritin cores indicated the presence of ferrihydrite ($5Fe_2O_3 \cdot 9H_2O$) of limited crystallinity. Phosphorus to iron atomic ratios were measured by ICP spectrometry. The phosphorus levels were close to the limit of detection, giving approximate mean values of P:Fe of 1:44 for the *P. laticostata* ferritin and 1:36 for the *A. hirtosa* ferritin. These levels of phosphate are significantly less than those for the crystalline cores of mammalian ferritins and considerably less than those for the noncrystalline core of bacterioferritins.

## Introduction

Chitons and limpets are marine invertebrates that incorporate iron minerals into composite materials that make up the hard structural components of the teeth on their radulas.[2,3] The radulas are used to scrape algae from the rocks in the intertidal regions and, in the process, are continuously worn away, thus necessitating the continual production of iron minerals to replace those lost with the discarded teeth. It has been suggested that this need for a high turnover of iron is related to the exceptionally high concentration (approximately 400 $\mu g \cdot mL^{-1}$) of ferritin found in the

[†] Murdoch University.
[‡] University of Bath.
[§] University of Liverpool.

(1) Present address: Department of Molecular Biology, College of Natural Sciences, Chonbuk National University, Chonju 560-756, Seoul, Korea.
(2) Lowenstam, H. A. *Science* **1981**, *90*, 1126.
(3) Webb, J. In *Biomineralization and Biological Metal Accumulation*; Westbroek, P., De Jong, E. W., Eds.; Reidel: Doredrecht, The Netherlands, 1983; pp 413-422.

0020-1669/90/1329-1870$02.50/0 